

PHYSICALLY FLEXIBLE MULTI-LAYER LIQUID METAL-BASED BAND-PASS METASURFACE

Arkadeep Mitra¹, Kevin Xu², Jun H. Choi², and Jeong-Bong Lee^{1*}

¹The University of Texas at Dallas, Richardson, Texas, USA

²University at Buffalo, Buffalo, New York, USA

ABSTRACT

A liquid metal-based physically flexible (stretchable, bendable, twistable, and foldable) thickness customized multi-layer second-order band-pass metasurface in the X-band (7 ~ 11.2 GHz) has been designed, fabricated, and characterized. The multi-layer metasurface consists of a liquid metal-based inverter layer in the middle to enable the metasurface extremely thin (total thickness of 4.81 mm, $< \lambda_0/7.5$). Liquid metal has been sprayed into the PDMS replicated patterns by using an airbrush operating at 36 psi. S-parameters of the metasurface sample measured using a WR-90 waveguide setup showed good agreement with simulated results.

KEYWORDS

PDMS, liquid metal, multi-layer, band-pass, flexible, stretchable, bendable, twistable, foldable, metasurface.

INTRODUCTION

Gallium-based liquid metals comprise of binary (e.g., EGaIn) or ternary (e.g., Galinstan) alloys of elements that fall under the zinc group in the periodic table [1]. In presence of oxygen, Galinstan (Ga: 68.5%, In: 21.5%, and Sn: 10%) forms 0.5~3 nm gallium oxide (Ga_2O_3 and Ga_2O) layer [1-2]. The viscoelastic gallium oxide coupled with high conductivities (electrical conductivity: 3.46×10^6 S/m at 20° C, thermal conductivity: 16.5 W/m-K at 20° C), low melting point (13.2° C), high boiling point of 1300° C, and low toxicity, when compared to mercury, makes it a favorable alternative [1, 3]. Galinstan when patterned in elastomeric polymers like polydimethylsiloxane (PDMS) (~160% maximum elongation) [4] and Ecoflex (~900% maximum elongation) [5] realizes a myriad range of physically flexible electronics applications ranging from electrocardiogram (ECG) to metasurfaces [3].

Metasurface-based frequency selective surfaces are spatial filters that exist in 1D or 2D as band-pass, band-stop, low-pass, and high-pass [6]. A metasurface comprises of artificially engineered man-made structures that transmit, reflect, or absorb electromagnetic (EM) waves of specific frequency bands [6]. A variety of metasurfaces have been demonstrated such as in spectral filters [7], high impedance surfaces [8], low-profile reflect arrays [9], and absorbers [10]. Metasurfaces are employed in radomes (terrestrial and airborne) [11-12], missiles [11], electromagnetic shielding [11], and Pico cellular wireless communication applications [13].

Liquid metal has been used in PDMS-based metasurfaces. However, previous liquid metal based metasurface works used surface mounting techniques for incorporation of chip resistors which makes it not flexible and/or liquid metal injection through continuous channels which significantly limits design flexibility of the metasurface [14-15]. We have demonstrated a single layer flexible band-stop metasurface using a massive array of discrete patterns of liquid metal which cannot be achievable with previous methods [3, 6]. In this work, we further extend our previous work to demonstrate an extremely thin physically flexible (stretchable, bendable, foldable, and twistable) multi-layer band-pass metasurface operating in the X-band.

DESIGN

The multi-layer metasurface consists of $m \times n$ array of modified Jerusalem cross frequency selective surface (FSS) resonator layers at the top and the bottom. Each unit cell of the FSS resonator has 300 μm wide, 4.3 mm long vertical and horizontal dipoles with 1 mm x 2 mm end cap which faces floating patch of the same size (Figure 1a). The top and bottom FSS resonator layers are inductively coupled through a liquid metal inverter layer in the middle with a square aperture (4.3 mm x 4.3 mm) that overlaps the horizontal and vertical dipoles of the resonators (Figure 1b).

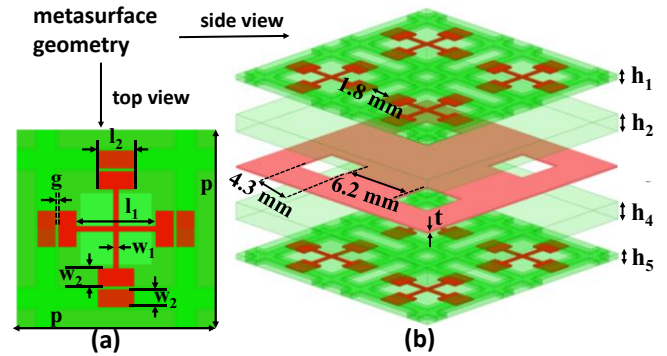


Figure 1. Schematic diagram of the multi-layer band-pass metasurface: (a) Top view of a unit cell: $l_2 = 2$ mm, $l_1 = 4.3$ mm, $w_1 = 0.3$ mm, $w_2 = 1$ mm, $g = 0.2$ mm, $p = 10.5$ mm, (b) 3D view of 2×2 cells: $t = 0.2$ mm, $h_1 = 0.7$ mm, $h_2 = 1.66$ mm, $h_4 = 1.55$ mm, $h_5 = 0.7$ mm.

The multi-layer metasurface (Figure 1b) have substrate thicknesses of $h_1 = 0.7$ mm, $h_2 = 1.66$ mm, $t = 0.2$ mm, $h_4 = 1.55$ mm, $h_5 = 0.7$ mm. The total thickness of the metasurface structure ($h = 4.81$ mm) is approximately $\lambda_0/7.5$, where λ_0 is the simulated finite array i.e., waveguide wavelength at 8.3 GHz.

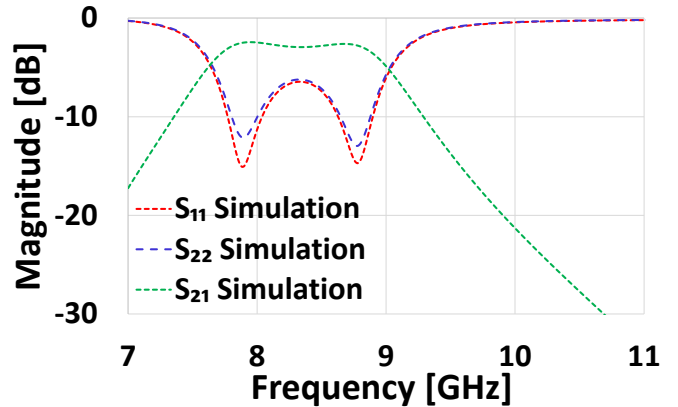


Figure 2. Simulated finite array band-pass metasurface results.

The metasurface comprising of PDMS (relative permittivity $\epsilon_r = 2.4$ and loss tangent $\tan \delta = 0.02$) as the non-conductive and the

uniformly thick ($t = 0.2 \text{ mm}$) (Figure 1b) liquid metal Galinstan as the conductive media (conductivity $\sigma = 3.46 \times 10^6 \text{ S/m}$), has been simulated as a finite array using ANSYS-HFSS (high-frequency structure simulator) which shows broad passing band around 8~9 GHz (Figure 2).

FABRICATION

A 4" inch silicon wafer was patterned with S1813 photoresist and Chromium hard-mask was deposited using e-beam evaporation. Followed by a hard mask deposition and resist lift-off, a plasma etch with C_4F_8 (75 sccm), SF_6 (100 sccm), Ar (30 sccm)

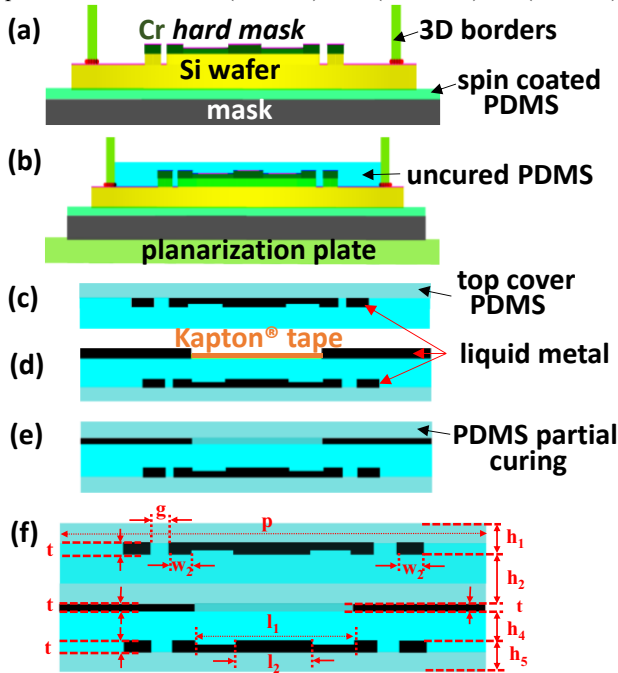


Figure 3. Fabrication sequence: (a) dry-etched Si mold, (b) PDMS replication, (c) top cover PDMS formation for encapsulation, (d) inverter layer liquid metal formation, (e) partially curing PDMS over the inverter layer, (f) top resonator layer aligned/bonded.

for 4 cycles (150 iterations/cycle; total iterations: 552) was done for dry etching of Si as per designed depth ($t = 0.2 \text{ mm}$). Teflon was deposited using C_4F_8 (75 sccm) and Ar (30 sccm) as a final step. The patterned Si mold was placed over a glass mask having spin coated uncured Sylgard 184 (Dow Chemical, Midland, MI, USA) 10:1 PDMS. Complete curing was done in a 95°C oven for 16 minutes. Followed by curing, a 3D printed border was placed along the edges of the mold and attached using Devcon epoxy (ITW Performance Polymers, Danvers, MA, USA). Reusability of the Si mold was ensured by these additional steps (Figure 3a).

The Si-mold structure was placed over a planarization plate. Uncured PDMS (10:1) was dispensed through a 1 mL syringe placed vertically centered over the mold and planarization was allowed for 24 hours at room temperature (Figure 3b). Following planarization curing was done on 96°C hotplate for 19 minutes. The cured top layer and bottom layer FSS-PDMS structures were placed over a cleanroom wipe. Galinstan (Changsha Rich Nonferrous Metals Co., Ltd., Hunan, China) mixed with 0.1 ml of 1% NaOH was sprayed into the patterns by using an airbrush (Paasche Airbrush Company, Kenosha, WI, USA) which operated at 36 psi, and was placed $\sim 20 \text{ cm}$ over the FSS-PDMS samples. Excess liquid metal outside of patterns were cleaned. A top cover

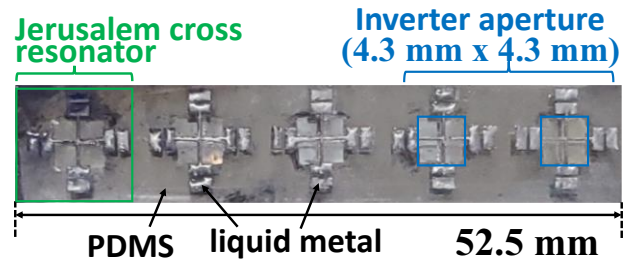


Figure 4. A photomicrograph of 1 x 5 fabricated band-pass metasurface

PDMS was further provided by dispensing through a 1 mL syringe and complete curing was allowed for approximately 48 hours at room temperature (Figure 3c).

The liquid metal patterned bottom FSS layer with protective top cover was flipped over and Kapton[®] tape (DuPont, Wilmington, DE) windows (4.3 mm x 4.3 mm) (Figure 3d) were placed overlapping the liquid metal patterned horizontal and vertical dipoles of the Jerusalem cross resonators. The Kapton[®] tape windows were fabricated by placement of four layers of Kapton tape (each layer measuring close to 55 microns) over the PDMS-inverter windows followed by cutting. The PDMS-inverter windows mold was replicated from the dry etched inverter-Si mold. Liquid metal mixed (1 mL) with 0.1 ml of 1% NaOH was sprayed over the collective inverter layer. Following spraying liquid metal planarization was done by placing a glass slide (5.08 cm x 7.62 cm x 0.1 cm) over the liquid metal and applying an external pressure. Following planarization completion, the glass slide was removed, and cleaning was done. For clear demarcation

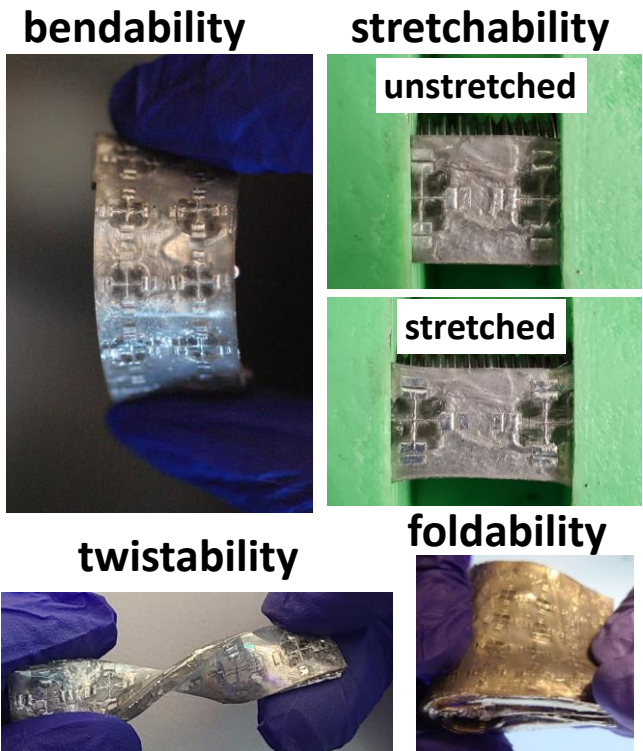


Figure 5. Physical flexibility demonstration of the fabricated metasurface.

of inverter layer window boundary, a very thin NeverWet® (Rust-Oleum Corp., Vernon Hills, IL, USA) layer (4.3 mm x 4.3 mm) was replaced after peeling away the Kapton-tape windows. The NeverWet® [16] skin in-turn was obtained by spraying into the 4.3 mm x 4.3 mm PDMS-inverter windows replicated from the inverter-Si mold. After cleaning and demarcation, the NeverWet® skin was removed. The inverter layer was sealed by dispensing uncured PDMS (10:1) through a 1 mL syringe. Partial curing of the PDMS was allowed for close to 22.5 hours at room temperature (Figure 3e), followed by which the dipoles of the top layer FSS (patterned with liquid metal and provided with protective top cover PDMS, Figure 3c) were aligned with that of the bottom layer FSS before placement on inverter layer. The integrated multi-layer structure ($h = 4.81$ mm) was cured for another 48 hours at room temperature (Figure 3f). Multiple versions of $m \times n$ band-pass metasurfaces were fabricated.

Figure 4 shows a 1×5 metasurface. Various versions of the fabricated metasurfaces were repeatedly tested for its bendability, twistability, stretchability, and foldability (Figure 5). No apparent damages on the metasurface were visible after more than 20 cycles of testing, a proof of its physical flexibility.

CHARACTERIZATION

Characterization was done in a waveguide environment (Figure 6) with targeted X-band (7 ~ 11.2 GHz) operation. A 1×2 metasurface was cut from the fabricated 1×5 metasurface. The metasurface was placed in an inner aperture of limited dimensions (10.16 mm x 22.86 mm), of the sample holder which was in-turn milled from the 6.35 mm thick Arconic MIC 6 cast aluminum sheet. The coaxial adapters acted as the interface between the Keysight N542A PNA-X network analyzer (Keysight Technologies, Santa Rosa, CA, USA) and the WR-90 waveguide (Pasternack, Irvine, CA, USA). Calibrations were performed up to the sample before measuring S-parameters.

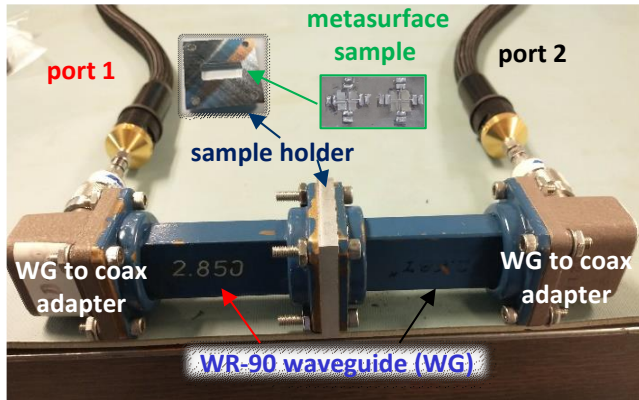


Figure 6. Waveguide characterization setup for the band-pass metasurface sample using WR-90 waveguide.

The measured S-parameters (Figure 7) results for the reflection and transmission of the multi-layer metasurface showed good agreement when compared with the simulation results (Figure 2). The center frequency of the measured and simulated sample was obtained at 8.325 GHz and 8.31 GHz, with a 3-dB fractional bandwidth of 12% and 17% respectively (Figure 7a).

CONCLUSION

In this work we demonstrated fabrication of multiple versions of physically flexible $m \times n$ band-pass metasurfaces. Spray coating was used for the discrete as well as continuous patterning of liquid

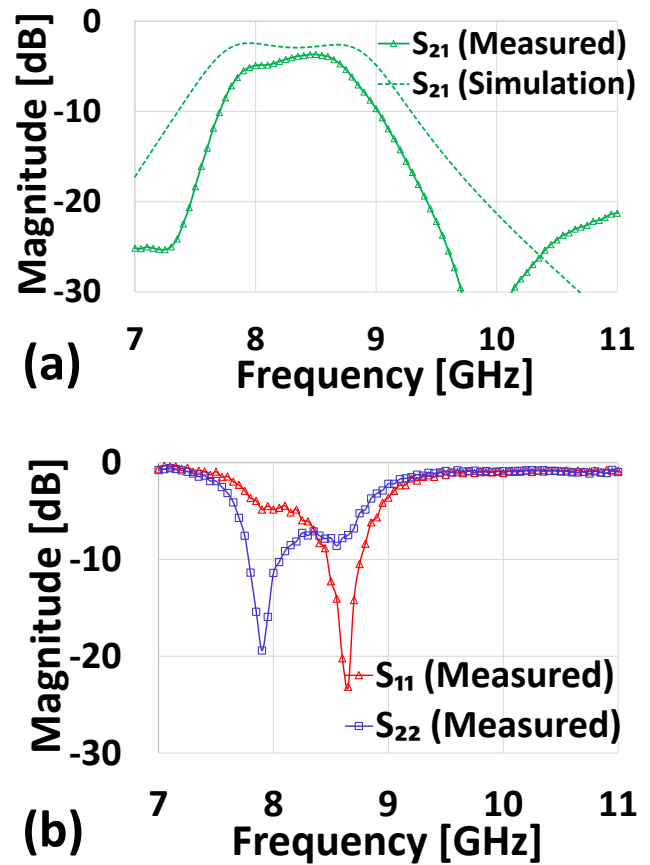


Figure 7. WR-90 waveguide results for band-pass metasurface. (a) Simulated and measured transmission coefficient. (b) Measured reflection coefficients.

metal in multiple PDMS layers. The waveguide simulation and measurement results showed good agreement.

We envision this unique, highly resilient physically flexible metasurface to be integrated in field-deployable metasurfaces uniquely suited for communication and military applications such as packable membrane reflectarrays for cargo space limited small satellites, and portable/rollable absorbers for on-demand deployment in stealth blanket operations. In practical applications, freezing point of liquid metal (e.g., at -19° C for Galinstan) [1] must be considered for storage and operation of the flexible metasurface to maintain its physical flexibility. In future works we envision to make the fixed floating patches dynamically tunable.

ACKNOWLEDGEMENTS

This work was supported in part by the United States National Science Foundation grant NSF ECCS-1908779. The authors would also like to acknowledge Dr. Ye Il Choi, Jinwon Jeong and UT Dallas Clean Room staff for their support on this work.

REFERENCES

- [1] T. Daeneke, K. Khoshmanesh, N. Mahmood, I.A. de Castro, D. Esrafilzadeh, S. J. Barrow, M.D. Dickey, and K. Kalantarzadeh, "Liquid metals: fundamentals and applications in chemistry", *Chemical Society Reviews*, 47, 4073 (2018).
- [2] D. Kim, P. Thissen, G. Viner, D.-W. Lee, W. Choi, Y.J. Chabal, and J.-B. Lee, "Recovery of nonwetting characteristics by surface modification of gallium-based

- liquid metal droplets using hydrochloric acid vapor”, *ACS Applied Materials & Interfaces*, 5, 179 (2013).
- [3] A. Mitra, K. Xu, S. Babu, J.H. Choi, and J.-B. Lee, “Liquid-Metal-Enabled Flexible Metasurface with Self-Healing Characteristics”, *Advanced Materials Interfaces*, 2102141 (2022).
- [4] L. Liang, and E. Ruckenstein, “Pervaporation of ethanol-water mixtures through polydimethylsiloxane-polystyrene interpenetrating polymer network supported membranes”, *Journal of Membrane Science*, 114, 227 (1996).
- [5] J.-B. Chossat, H.-S. Shin, Y.-L. Park, and V. Duchaine, “Soft Tactile Skin Using an Embedded Ionic Liquid and Tomographic Imaging”, *Journal of Mechanisms and Robotics*, 7, 021008 (2015).
- [6] A. Mitra, K. Xu, S. Babu, J.H. Choi, and J.-B. Lee, “Liquid Metal-Based Flexible Band-Stop Frequency Selective Surface”, 2021 IEEE 34th International Conference on Micro Electro Mechanical Systems (MEMS), Gainesville, FL, 1/25-29/22, IEEE, 2021, pp. 953-956.
- [7] A.E. Minovich, A.E. Miroschnichenko, A.Y. Bykov, T.V. Murzina, D.N. Neshev, and Y.S. Kivshar, “Functional and nonlinear optical metasurfaces”, *Laser & Photonics Reviews*, 9, 195 (2015).
- [8] A. Vallecchi, R.J. Langley, and A.G. Schuchinsky, “Metasurfaces With Interleaved Conductors: Phenomenology and Applications to Frequency Selective and High Impedance Surfaces”, *IEEE Transactions on Antennas and Propagation*, 64, 599 (2016).
- [9] J. Wang, Y. Li, Z.H. Jiang, T. Shi, M.-C. Tang, Z. Zhou, Z.N. Chen, and C.-W. Qiu, “Metantenna: When Metasurface Meets Antenna Again”, *IEEE Transactions on Antennas and Propagation*, 68, 1332 (2020).
- [10] K. Payne, K. Xu, JH Choi, and JK Lee, “Plasma-Enabled Adaptive Absorber for High-Power Microwave Applications”, *IEEE Transactions on Plasma Science*, 46, 934 (2018).
- [11] R.S. Anwar, L. Mao, and H. Ning, “Frequency Selective Surfaces: A Review”, *Applied Sciences*, 8, 1689 (2018).
- [12] E. Ahamed, M.R.I. Faruque, M.F.B. Mansor, and M.T. Islam, “Polarization-dependent tunneled metamaterial structure with enhanced fields properties for X-band application”, *Results in Physics*, 15, 102530 (2019).
- [13] T.Z. Fadhil, N.A. Murad, M.K.A. Rahim, M.R. Hamid, and L.O. Nur, “A Beam-Split Metasurface Antenna for 5G Applications”, *IEEE Access*, 10, 1162 (2021).
- [14] S. Ghosh, and S. Lim, “Fluidically reconfigurable multifunctional frequency-selective surface with miniaturization characteristic”, *IEEE Transactions on Microwave Theory and Techniques*, 66, 3857 (2018).
- [15] H.K. Kim, D. Lee, and S. Lim, “Wireband-Switchable Metamaterial Absorber Using Injected Liquid Metal”, *Scientific Reports*, 6, 31823 (2016).
- [16] I.D. Joshipura, H.R. Ayers, G.A. Castillo, C. Ladd, C.E. Tabor, J.J. Adams, and M.D. Dickey, “Patterning and Reversible Actuation of Liquid Gallium Alloys by Preventing Adhesion on Rough Surfaces”, *ACS Applied Materials & Interfaces*, 10, 44686 (2018).

CONTACT

*Jeong-Bong (JB) Lee, tel: +1-972-658-6750; jblee@utdallas.edu